Hyperfine Interactions 76 (1993) 205–220

Trapping and cooling of (anti)hydrogen

J.T.M. Walraven

Van der Waals–Zeeman Laboratory, University of Amsterdam, Valckenierstraat 65–67, 1018 XE Amsterdam, The Netherlands

Magnetic traps offer the possibility for long-term storage and accumulation of atomic antihydrogen. These are invaluable features for revealing subtle differences that may exist between hydrogen and antihydrogen in interaction with electromagnetic or gravity fields. An overview is given of various aspects associated with trapping and cooling of neutral particles, putting emphasis on their relevance for the antihydrogen problem.

1. Introduction

It is a fascinating thought that it may be possible in the not too distant future to study the simplest form of atomic antimatter, antihydrogen, within the walls of a physics laboratory. The essential ingredients are at our disposal. Antiprotons are being manipulated routinely at CERN and stored for essentially arbitrarily long periods in a Penning trap to search for subtle asymmetries in its behaviour compared to that of the proton [1–4]. Positrons are familiar already for a long time in many fields of physics and manipulated in laboratories all over the world [5]. Clearly, the present challenge is to combine these particles into the antiparticle of the hydrogen atom (H), i.e. to create antihydrogen ($\bar{H}$) [6,4].

There is no a priori theoretical reason to expect dramatic differences in behavior between H and $\bar{H}$ in interaction with electromagnetic or gravity fields. However, the observation of *any* asymmetry in this respect, whatever small, has profound consequences for the fundamental understanding of matter [7]. The experimental efforts to create $\bar{H}$ are therefore best directed towards methods that allow, in due time, for precision experiments in the electromagnetic and gravitational domain. Building on the experience with trapped antiprotons [1–3] and trapped atomic hydrogen [8–13], the use of a neutral atom trap appears the logical choice for future experiments with $\bar{H}$.

Traps offer the possibility for long term storage and accumulation of $\bar{H}$ and, at sufficient density, even for the containment of $\bar{H}$ in a gaseous state in internal thermal equilibrium. In a trap it seems also feasible to mix samples of H and $\bar{H}$ and to study $\bar{H}$–H collisions by observing the annihilation decay as a function of time [14].

Also the subkelvin temperatures (translational energies) characteristic for trapped neutral atoms are desireable from the experimental point of view. For the spectroscopist the atoms cannot move slowly enough [15–17]. The lifetime of the metastable $2\,^2S_{1/2}$ state is extremely long (1/7 s). The resolution of Doppler-free two-photon spectroscopy of the $1\,^2S_{1/2} \rightarrow 2\,^2S_{1/2}$ transition, used for precision determinations of the Rydberg, is limited by second-order Doppler broadening which scales (for a thermal sample) linearly with temperature T ($\Delta\omega/\omega = -\frac{1}{2}v^2/c^2 \propto T$, where ω is the transition frequency, v is the thermal speed and c is the speed of light) and shows up in an asymmetric lineshape. Hänsch and co-workers [18] recently obtained a width of ~ 9 kHz for these lines using a cryogenic atomic beam operated at $T \approx 9$ K. Hence, it should be possible to virtually eliminate second order Doppler broadening by using magnetically trapped atoms at temperatures of a few millikelvin [16,17].

It is also instructive to compare the temperature of trapped atoms with the gravitational energy. Due to the small mass of $\bar{H}$, a 1 m difference in gravitational height corresponds to a potential energy difference of only ~ 1 mK. Hence, direct measurements of the gravitational acceleration by ballistic methods become possible at temperatures of order 1 mK or below [19,20]. With regard to conceivable studies of $\bar{H}$–H collisional properties it is appropriate to mention that the quantum regime (s-wave scattering limit) is reached for $T \lesssim 1.5$ K [14].

2. Trapping neutral particles

To trap a neutral particle two essential conditions have to be satisfied. First the particle has to be slowed down to a trapable kinetic energy, i.e. a kinetic energy smaller than the potential well depth of the trap being used (typically ~ 1 K). Then, to realize the actual trapping, an additional requirement is essential. It clearly is not sufficient to simply present a static trapping potential to the particle as this only leads to a reversible exchange of kinetic and potential energy during the passage of the particle over the trap. Some dissipation mechanism is needed, although this may be avoided by a trick such as rapidly switching the trapping field, catching a bunch of particles while they reside in the trapping region.

The first neutral particle to be trapped was the neutron. Kügler et al. [21] injected a beam of slow neutrons ($v < 20$ m/s) into a 1.2 m diameter magnetic storage ring with the aid of a pneumatically driven totally reflecting mirror. By rapidly withdrawing the mirror before the neutrons complete their first full revolution trapping could be realized.

Trapping of neutral atoms proceeds quite differently. Migdall et al. [22] used an atomic beam of Na atoms which was slowed down by a counter-propagating laser beam using optical (Doppler) cooling with the Zeeman-tuning technique [23], in which a tapered magnetic field serves to compensate for the changing Doppler shift during the slow down. Trapping was realized by rapidly energizing a two-coil

minimum-B-field trap, catching only those atoms that happen to reside in the trapping region at the instant the trap is closed (single bunch method).

Continuous loading of Na into a static trap was first realized by Bagnato et al. [24]. In this experiment the oscillatory motion in a minimum-B-field trap of the type proposed by Pritchard [25] was damped by applying a one-dimensional optical molasses [26] along the axis of the trap.

Trapping experiments with H were done at MIT in the group of Greytak and Kleppner [8,10,11] and in the Van der Waals–Zeeman laboratory of the University of Amsterdam [9,12,13]. In principle, also H can be cooled and trapped with the optical methods mentioned above, but unfortunately the appropriate light source, a cw laser at wavelength $\lambda = 121.6$ nm to excite the $1\,^2S \rightarrow 2\,^2P$ transition (Lyman-α; L_α) is not available. Interestingly enough, H happens to be the only atomic system that may be cooled and trapped with a non-optical method. As originally demonstrated at the University of Amsterdam [27], H can be cooled to subkelvin temperatures by exchanging heat with liquid helium covered surfaces. Hess [28] proposed to exploit this feature to both cool and trap H, relying on interatomic collisions in the trap to dissipate the kinetic energy of the accelerated particles into heat (heat of trapping). Hess et al. [8] reported the first experiments based on this approach.

Not surprisingly, also antihydrogen requires its tailor-made approach. The method to cool H cannot be applied to $\bar{H}$ due to the large probability of annihilation of the anti-atom in a surface collision. Also the optical cooling and trapping methods seem out of reach [29,30]. In the case of $\bar{H}$, however, we have the interesting option to synthesize the anti-atom inside the magnetic trap. For this it is essential that the formation process does not result in $\bar{H}$ atoms having a translational energy that exceeds the well depth of the trap (~ 1 K). Starting with antiprotons ($\bar{p}$) and positrons (e^+) or positronium (Ps), three formation mechanisms are discussed in the literature [6,4],

$$\begin{aligned} &\bar{p} + 2e^+ \rightarrow \bar{H}^* + e^+, \\ &\bar{p} + Ps^* \rightarrow \bar{H}^* + e^-, \\ &\bar{p} + e^+ + n\hbar\omega \rightarrow \bar{H}^* + (n+1)\hbar\omega. \end{aligned} \tag{1}$$

These processes are known as the three-body recombination mechanism, the exchange reaction with excited positronium and stimulated photorecombination, respectively. Starting with the constituent particles at rest, the $\bar{H}^*$ should be created in an excited state with sufficiently large principle quantum number if the formation recoil (of the first two processes due to ejection of the e^+ or e^-) is to be less than 1 K. It should be noted in this context that if the $\bar{H}^*$ is created with substantial electronic orbital angular momentum the effective trapping depth may be substantially larger than 1 K, making the trapping easier. Further, the projection of the magnetic moment on the magnetic field vector should not change sign during de-excitation to the ground state. The duration of the de-excitation time seems of

little concern in view of the exceptionally long holding times that may be achieved in a cryogenic environment.

3. Magnetic traps

Static magnetic traps are currently being used in trapping experiments with H [8–13]. This type of trap is based on the spatial dependence of the Zeeman energy $E_Z = -\boldsymbol{\mu}\cdot\boldsymbol{B}(\boldsymbol{r})$ of a neutral particle with magnetic moment $\boldsymbol{\mu}$ in an inhomogeneous magnetic field $\boldsymbol{B}(\boldsymbol{r})$. Particles with their magnetic moments polarized anti-parallel to the local magnetic field experience an effective potential well

$$U_p(\boldsymbol{r}) = \mu[B(\boldsymbol{r}) - B_0] \tag{2}$$

around a magnetic field minimum B_0 (minimum in the modulus $B(\boldsymbol{r})$ of the magnetic field) in which they remain trapped if their kinetic energy is insufficient to reach the edge of the well. Magnetostatic traps are always based on magnetic field minima as a local magnetic field maximum in free space is inconsistent with the Maxwell equations [31]. For a Bohr magneton, such as in the case of $\bar{H}$, the trapping energy is 0.67 K/T. This implies that for superconducting magnets of typically several tesla a magnetic well depth of at most a few kelvin may be realized.

It should be emphasized that also interesting dynamic confinement principles have been proposed to trap H. Lovelace et al. [32] proposed an ac magnetic trap formed by superimposing a large static field and a low frequency ($\sim$ 1 kHz) oscillatory field generated by a coil having its symmetry axis along the direction of the main field. This trap operates on the same dynamical confinement principle as the Paul trap for ions [33]. Although originally proposed for H, this trapping principle was first implemented experimentally for cesium by Cornell et al. [34]. The rather small trapping depth ($\sim$ 1 mK) that may be realized with this approach is incompatible with the cryogenic filling technique used with H.

Agosta and Silvera devised a resonant microwave trap, based on trapping of permanent magnetic dipole moments in the focal region of a concentric microwave etalon located in a homogeneous magnetic field [35]. Driving the dipoles at a (near)resonant frequency they experience a spatially inhomogeneous effective magnetic field (Rabi field). Particles with magnetic moments having a positive projection onto the Rabi field direction are pulled into the focal region, those with a negative projection are repelled. Depending on the detuning, the trapped states have their magnetic moment mostly parallel (negative detuning) or antiparallel (positive detuning) with respect to the homogeneous field. The principle of this trap, also originally proposed for H, was recently demonstrated for cesium at NIST [36]. Like the low frequency ac trap also the resonant microwave trap is rather shallow, typically a few mK.

Let us now return to the static magnetic traps and analyze the choice of trap for the H experiments. A careful review of static trap field configurations has been

given by Bergeman et al. [37]. The simplest magnetostatic trap is the two-coil quadrupole trap. Two dipole coils, wound in opposite direction, produce a highly inhomogeneous field with a characteristic zero-field point in the center. As the potential does not depend on the azimuthal angle (ϕ) the orbital angular momentum along the trap axis is conserved. Strictly speaking, this is only true if the atomic magnetic moment adiabatically follows the changing direction of the magnetic field along the orbit. If the atoms pass near the zero field region, i.e. for small angular momentum along the z-axis, Majorana depolarization (spin flips) may occur which leads to ejection of the particles from the trap. In the collisionless regime this leads to depletion of the fraction of particles with small angular momentum along the
z-axis. In general this fraction is small, except for conditions where only the low lying oscillator levels in the trap are populated (for H this requires energies below ~ 1 mK). For the two-coil quadrupole the problem of Majorana depolarization has been analyzed in detail for the collisionless regime by Bergeman et al. [38].

Trapping experiments with H are done at densities $10^{11} \lesssim n_H \lesssim 10^{14}\,\mathrm{cm}^{-3}$. At such densities thermalization occurs within a few seconds (see section 4). The low-lying oscillator states, most susceptible to Majorana depolarization, are therefore continuously replenished which results in a steady loss of sample. For the experiments with H, aimed at observing a macroscopic population of the ground oscillator due to Bose–Einstein condensation, this effect is clearly unacceptable. Therefore, the zero-field point is avoided by choosing the Ioffe geometry, two coils with parallel current in combination with four straight conductors (Ioffe bars) biased to produce a quadrupole field (note that adding a homogeneous field to the two-coil quadrupole field only leads to a shift in the position of the field zero). The Ioffe trap was originally proposed for plasma confinement [39]. Its importance for neutral atom trapping was pointed out by Pritchard [25].

The coil arrangement, sample cell and field profile of the Ioffe trap used in Amsterdam are shown in fig. 1 [9,12,13]. The trapping field is generated by four dipole coils, having a common symmetry axis (z-axis), and four racetrack shaped coils parallel to this axis. The field minimum arises as the sum of a dipole field, due to the dipole coils and mainly directed along the symmetry axis and a quadrupole field produced by the racetracks and purely orthogonal to the z-axis. The two dipole coils in the middle are used to trim the field near the field minimum. The use of four racetrack coils rather than two assures a pure quadrupolar symmetry all along the symmetry axis. Near the trap minimum the field may be expressed to good approximation by the following expression in cylindrical coordinates:

$$\begin{aligned} B_\rho &= -\alpha\rho\cos 2\phi - \beta\rho z, \\ B_\phi &= \alpha\rho\sin 2\phi, \\ B_z &= B_0 + \beta z^2 - \tfrac{1}{2}\beta\rho^2. \end{aligned} \tag{3}$$

The modulus of the magnetic field is given to good approximation by

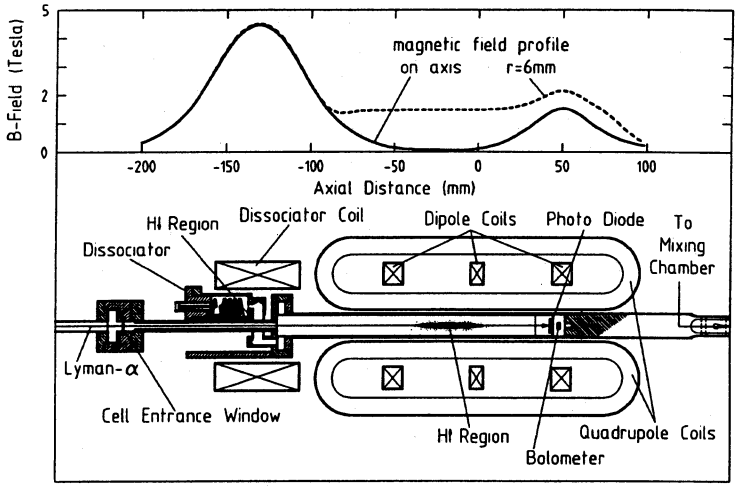

Fig. 1. The Ioffe trap used in Amsterdam with corresponding field profile. Solid line: field along the axis; dashed line: field 6 mm off-axis (on wall of sample cell).

$$B = \sqrt{(B_0 + \beta z^2)^2 + (\alpha^2 - 2\alpha\beta z \cos 2\phi)\rho^2}. \tag{4}$$

The $\cos 2\phi$ term in eq. (4), due to the quadrupole field, breaks the axial symmetry around the trap axis. Therefore, unlike the two-coil quadrupole the Ioffe configuration does not conserve the orbital angular momentum along the trap axis although the violation is small for orbits confined to small values of z. The coupling between the three degrees of freedom in the motion of atoms trapped in this type of trap is discussed by Shlyapnikov et al. [14].

4. Stability considerations

To clarify the limitations on the stability of $\bar{H}$ in a magnetic trap, let us discuss a typical experiment with ordinary H. To have a complete picture the full experimental cycle is discussed, although the filling stage is not relevant for the $\bar{H}$ case. The H atoms are produced by dissociating solid H_2 in a helical rf cavity operated at 0.6 K in a $\sim$ 4 T magnetic field (see fig. 1). Helium provides an exceptionally small energy of physisorption (ε_a) to the H atom, $\varepsilon_a \approx 1$ K for H on ^{4}He and $\varepsilon_a \approx 0.4$ K for H on ^{3}He. Therefore, to minimize sample loss due to surface catalyzed recombination, the walls of the sample cell and dissociator are covered with a film of liquid helium. All four hyperfine states of the $1\,^2S_{1/2}$ electronic ground state are produced in the dissociation process. These are labeled a, b, c and d in order of increasing energy (see fig. 2) and may be expressed as linear combinations of the high field basis states $|m_s, m_i\rangle$:

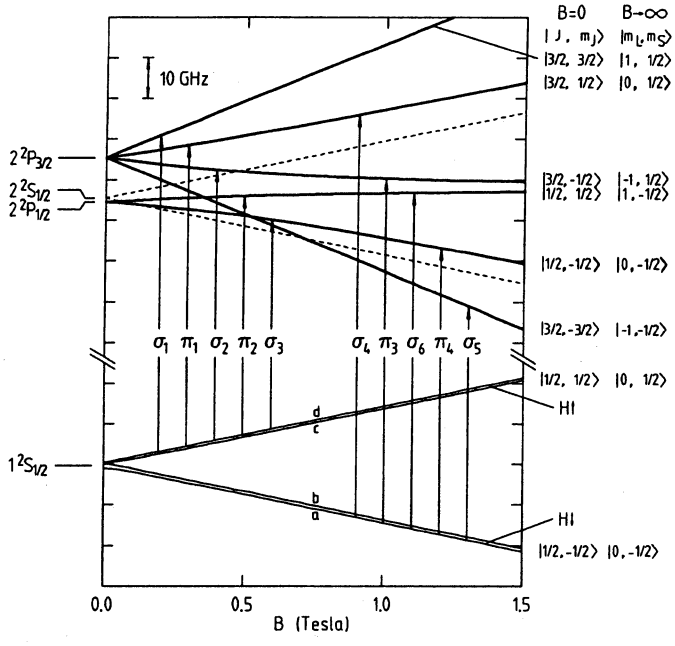

Fig. 2. Fine structure diagram of atomic hydrogen. For the ground state the hyperfine structure is also shown.

$$|d\rangle = |\uparrow\uparrow\rangle, \quad |c\rangle = \cos\theta|\uparrow\downarrow\rangle + \sin\theta|\downarrow\uparrow\rangle,$$
$$|b\rangle = |\downarrow\downarrow\rangle, \quad |a\rangle = \sin\theta|\uparrow\downarrow\rangle - \cos\theta|\downarrow\uparrow\rangle, \tag{5}$$

where the hyperfine mixing angle θ is defined by $\tan 2\theta \equiv a_h/[\hbar(\gamma_e + \gamma_p)B]$, with a_h the hyperfine constant and $\gamma_e = 1.760 \times 10^{11}\ s^{-1}\ T^{-1}$ and $\gamma_n = 2.675 \times 10^8\ s^{-1}\ T^{-1}$ the electron and proton gyromagnetic ratios, respectively.

The gas distributes itself over the cell in accordance to the electron-spin polarization. The atoms in c and d states (H $\uparrow$) are pulled into the trapping region (low-field seekers) and thermalize, whereas a- and b-state atoms (H $\downarrow$) remain near the dissociator (high-field seekers). In thermal equilibrium the density distribution of H $\uparrow$ (or $\bar{\text{H}}\downarrow$) as a function of position $\boldsymbol{r}$ may be written as

$$n(\boldsymbol{r}) = n_0 \exp[-U_p(\boldsymbol{r})/k_B T], \tag{6}$$

where n_0 is the density at the center of the trap. With the trapped gas effective volumes of order $l = 1, 2, 3, \ldots$ are associated, which are defined by

$$V_{le} = \int [n(\boldsymbol{r})/n_0]^l \, d\boldsymbol{r}. \tag{7}$$

Notice that $V_{le}(T) = V_{1e}(T/l)$, $V_{1e} = N/n_0$. At low temperatures the density of trapped gas near the walls is negligible and V_{1e} may be expressed in approximate form as

$$V_{1e} = V_0[1 + \tfrac{3}{2}(T/T_0)](T/T_0)^{3/2}, \tag{8}$$

with $V_0 = 2\pi^{3/2}\alpha^{-2}\beta^{-1/2}B_0^{5/2}$, and $T_0 = \mu_B B_0/k_B$. For the Ioffe trap used by Luiten et al. [12] $V_0 = 0.048\,\mathrm{cm}^3$ and $T_0 = 67\,\mathrm{mK}$. Knowledge of V_{1e} and its temperature dependence is essential for a detailed description of many of the (quasi)equilibrium properties of the trapped gas.

As an estimate for the characteristic time for internal thermalization we calculate the elastic collision *event* rate τ_c^{-1} per atom. For a gas in thermal equilibrium

$$\tau_c^{-1} = n_0 G_{el} V_{2e}/V_{1e}, \tag{9}$$

where $G_{el} \equiv \frac{1}{2}\bar{v}_r\sigma_{el}$ is the event rate constant with $\sigma_{el} = 1.3 \times 10^{-15}\,\mathrm{cm}^2$ the elastic (s-wave) cross section and $\bar{v}_r = [16k_BT/\pi m]^{1/2}$ the average relative thermal speed. For $n_0 = 10^{12}\,\mathrm{cm}^{-3}$ and $T = 100\,\mathrm{mK}$ one calculates $\tau_c \approx 2\,\mathrm{s}$.

The stability of H ↑ gas is limited by magnetic relaxation to H↓, caused by spin exchange and the magnetic dipolar interaction between the atoms. The rates for these processes have been calculated by Lagendijk et al. [40] and Stoof et al. [41]. Spin exchange is a very efficient mechanism. However, for only collisions between two *c*-state atoms it leads to relaxation, provided the mixing angle θ is not too small. In collisions between two *d*-state atoms spin exchange is trivially of no consequence as is seen from eq. (5). For *c–d* collisions one may show that spin-exchange relaxation may proceed only via odd partial waves which are not populated in the s-wave scattering limit. Hence, in the case of *d–d* and *c–d* collisions, relaxation proceeds much slower because it is induced by the relatively weak dipolar interaction. For a mixture of *c* and *d* state atoms this implies a depletion of the *c*-state component and spontaneous electronic *and* nuclear polarization of the samples [40].

We estimate the lifetimes for both relaxation processes. For a pure *d*-state sample the decay rate $\tau_{dip}^{-1} \equiv \dot{N}/N$ due to dipolar relaxation is given by

$$\tau_{dip}^{-1} = n_0\langle G_{dd}\rangle V_{2e}/V_{1e}, \tag{10}$$

where $\langle G_{dd}\rangle$ is the *loss* rate constant for dipolar relaxation averaged over the trap according to $\langle G\rangle \equiv (1/V_{2e})\int G(\boldsymbol{r})[n(\boldsymbol{r})/n_0]^2\,\mathrm{d}\boldsymbol{r}$. In terms of the *event* rates defined in ref. [41] G_{dd} may be expressed as $G_{dd} = 2G^d_{ddaa} + G^d_{ddac} + G^d_{ddad}$. For the trap used by Setija et al. [13] with $n_0 = 10^{12}\,\mathrm{cm}^{-3}$ and $T = 10$ mK the average yields $\langle G_{dd}\rangle \approx 2 \times 10^{-15}\,\mathrm{cm}^3/\mathrm{s}$ and $\tau_{dip} = 1000$ s. Similarly, for a pure *c*-state sample under the same conditions but for spin exchange $G_{cc} = 2G^c_{ccaa} + G^c_{ccac} + G^c_{ccbd}$ $\approx 10^{-13}\,\mathrm{cm}^3/\mathrm{s}$ and $\tau_{ex} \approx 20\,\mathrm{s}$.

Clearly the description given above for H can be reformulated for $\bar{\mathrm{H}}$ simply by reversing all spins in eq. (5). Both the thermalization rate and the relaxation rates will be identical to the H case. As an example assume that $N = 10^6$ anti-atoms atoms are somehow trapped and cooled to 10 mK in a trap with the same parameters as the Ioffe trap used in Amsterdam[#1]. With eq. (8) the effective volume is

[#1] Trap parameters used in refs. [12,13]: $B_0 = 0.1$ T, $\alpha = 2.2$ T/cm, $\beta = 0.022\,\mathrm{T/cm}^2$, $V_0 = 0.048\,\mathrm{cm}^3$ and $T_0 = 67$ mK.

found to be $V_{1e} = 3.4 \times 10^{-3}\,\mathrm{cm}^3$ and $n_0 = 3 \times 10^8\,\mathrm{cm}^{-3}$. Thus, with $G_{el} = 1.3 \times 10^{-12}\,\mathrm{cm}^3/\mathrm{s}$ (see above) at 10 mK, one calculates $\tau_c^{-1} = 1.3 \times 10^{-4}\,\mathrm{s}^{-1}$ which means that the sample thermalizes in approximately 2 h. Similarly, with the rate constant for spin exchange ($G_{cc} \approx 10^{-13}\,\mathrm{cm}^3/\mathrm{s}$) the $\bar{\mathrm{H}}$ sample is found to be depleted from the c-state fraction in approximately one day. The dipolar lifetime of the sample is calculated to be 2 months. Hence, after storage for 24 h at 10 mK in an appropriate Ioffe trap an $\bar{\mathrm{H}}$ sample with behave as a (meta)stable gas in internal thermodynamic equilibrium. However, assuming in a less optimistic scenario that "only" $N = 10^4$ anti-atoms are trapped the sample is better described, even after several days at 10 mK, as a collection of non-interacting particles.

5. Evaporative cooling

Several methods are described in the literature that may be applied to cool, at least in principle, magnetically trapped $\bar{\mathrm{H}}$. Two of the methods, evaporative cooling and optical cooling, have been demonstrated with magnetically trapped H and will be discussed in the coming two sections. Other methods are adiabatic cooling and cooling by mixing $\bar{\mathrm{H}}$ into H. These are described by Shlyapnikov et al. [14] elsewhere in this volume.

Evaporative cooling was proposed in 1985 by Hess [28] and has been applied most successfully at MIT in the group of Greytak and Kleppner and co-workers, who reached temperatures down to 100 μK with this method in H gas [8,10,11]. Recently, in a spectroscopic study of magnetically trapped H, evaporative cooling was studied optically by Luiten et al. [12] at the University of Amsterdam. An optical variant of evaporative cooling, light induced evaporation (LIE), was demonstrated very recently by Setija et al. [13]. LIE is not further discussed in this paper as it only can be applied at densities $n_0 \gtrsim 10^{13}\,\mathrm{cm}^{-3}$ which seem unrealistically high for $\bar{\mathrm{H}}$.

Evaporative cooling is based on the selective removal of atoms with a (total) energy which is higher than the average. It is essential that the atoms are removed under quasi-equilibrium conditions, i.e. at a rate τ_e^{-1} slow in comparison to the elastic collision rate τ_c^{-1} (thermalization rate) but faster than the sample decay rate τ_d^{-1}. The internal energy of the gas is given by

$$U = (\gamma_{1e} + \tfrac{3}{2}) N_B T, \tag{11}$$

as the sum of a potential energy (first term) and a kinetic energy (second term) contribution. In analogy with eq. (7) it is useful to define potential energy averages of order $l = 1, 2, 3, \ldots$

$$\gamma_{le} k_B T = V_{le}^{-1} \int U_p(r) [n(r)/n_0]^l \, \mathrm{d}r. \tag{12}$$

Notice that $\gamma_{le}(T) = \gamma_{1e}(T/l)/l$ and $\gamma_{1e}(T) = (T/V_{1e})(\partial V_{1e}/\partial T)$. If atoms are allowed to escape (evaporate) over a potential energy barrier of height $\epsilon_{tr} \equiv \eta k_B T$, then the rate of change of internal energy of the sample is

$$\dot{U} = (\eta + \tfrac{3}{2})\dot{N}_B T. \tag{13}$$

Combining eqs. (11) and (13) leads to the following relationship between temperature and total particle number:

$$\frac{\dot{T}}{T} = \frac{\eta - \gamma_{1e}}{\gamma_{1e} + T(\partial\gamma_{1e}/\partial T) + \frac{3}{2}} \frac{\dot{N}}{N}. \tag{14}$$

Thus for $\eta > \gamma_{1e}$ particles loss leads to cooling. For a fixed value of ϵ_{tr} the η increases with decreasing temperature ($\eta \propto 1/T$) and the evaporation rate

$$\tau_e^{-1} \approx \tau_c^{-1} e^{-\eta} \tag{15}$$

is suppressed exponentially. Therefore, to continue the evaporation at constant rate, ϵ_{tr} has to be ramped-down in order to keep η constant. This procedure is known as forced evaporative cooling [10,11]. For the Ioffe trap used in Amsterdam one easily derives that $\frac{3}{2} \leqslant \gamma_{1e} \leqslant \frac{5}{2}$ and $T(\partial\gamma_{1e}/\partial T) \ll \gamma_{1e} + \frac{3}{2}$. Using the identities $\dot{N}/N = \dot{n}_0/n_0 + \dot{V}_{1e}/V_{1e}$ and $\dot{V}_{1e}/V_{1e} = \gamma_{1e}\dot{T}/T$, it is found that, in spite of the particle loss, the central density may *increase* according to

$$\frac{\dot{n}_0}{n_0} = \frac{\gamma_{1e}^2 + (1-\eta)\gamma_{1e} + T(\partial\gamma_{1e}/\partial T) + \frac{3}{2}}{\eta - \gamma_{1e}} \frac{\dot{T}}{T}. \tag{16}$$

The steepest increase in n_0 is obtained for $n \to \infty$ (which corresponds to the limit of constant particle number). The other limit, $\eta \to 0$, implies both heating and loss of n_0. Magnetic relaxation relates to an intermediate case in which atoms are removed at an average potential energy $\eta_{rel} k_B T = \gamma_{2e} k_B T$. Because in general $\gamma_{2e} < \gamma_{1e}$ the relaxation always leads to heating. For the Ioffe trap used in Amsterdam (see footnote #1 above) $\gamma_{1e} \approx \frac{3}{2}$ and $\eta_{rel} \approx \gamma_{1e}/2$.

Let us now turn to the consequences for antihydrogen. $\bar{H}$ can be cooled evaporatively if the samples can be made sufficiently dense to achieve thermal equilibrium. As discussed in previous section this is possible with $N = 10^6$ atoms at 10 mK in a Ioffe trap as used in Amsterdam (footnote #1). To cool the sample by forced evaporation at constant n_0 one has to choose $\eta \approx 3.5$ as follows from eq. (16) by setting $\dot{n}_0 = 0$. With the aid of eqs. (14) and (15) the cooling rate is then found to be $\dot{T}/T \approx \frac{4}{3}\tau_e^{-1} = 4 \times 10^{-2}\tau_c^{-1}$. Since this rate may be impractically slow one could aim for cooling with increasing n_0, which, although initially slower, at least becomes faster with decreasing temperature. A more practical approach is to select a trap with a smaller effective volume. With the Ioffe traps V_{1e} may be reduced by increasing the β parameter and decreasing B_0 (see eq. (8); it is hard to improve on the α parameter). The V_{1e} of the configuration used by van Roijen et al. [9] is, at 10 mK, a factor 4 smaller than the value used in the example. The trap configurations used at MIT were optimized to yield a large effective volume [8,10,11].

6. Optical cooling

Optical cooling of trapped $\bar{H}$ should be possible using a well-established deceleration principle based on the Doppler effect (Doppler cooling) [42–44]. Relatively few papers deal with optical cooling of magnetically trapped neutral atoms. Helmerson et al. [45,46] studied the case of Na. The hydrogen case was analyzed by Hijmans et al. [47]. Very recently Setija et al. [13] succeeded in demonstrating Doppler cooling of H experimentally. Doppler cooling of ground state H atoms requires excitation of the $1\,^2S \rightarrow 2\,^2P$ transition (Lyman-α) by a narrow band light source in the vacuum ultraviolet (VUV). Starting from the d state there are five allowed electric dipole transitions, labeled $\sigma_1, \pi_1, \sigma_2, \pi_2$ and σ_3 in the notation of Hijmans et al. [47] (see fig. 2). For c-state atoms also the $2\,^2P_{3/2,m_J=-3/2}$ state may be excited due an electron-spin-down admixture in low field caused by the hyperfine interaction (see eq. (5)). Only the σ_1 transition corresponds to a closed optical pumping cycle (for d-state atoms). All other transitions have branching ratios that lead to H↓. To enable Doppler cooling with minimal optical pumping losses (0.3% per scattered photon for d-state atoms) the σ_1 transition is spectrally isolated from the other transitions by applying a small offset field $B_0 = 0.1$ T.

The optical requirements put severe practical limitations on the experimental possibilities [29,47]. The light source of Setija et al. [13] is based on nonresonant third-harmonic generation of L_α using frequency-doubled, pulse-amplified light from a tunable cw dye-laser operated at 729.4 nm. Detailed descriptions are given elsewhere [47,48]. The source yields typically $2 \times 10^9 L_\alpha$ photons per 10 ns pulse in a bandwidth of 100 mHz and at a repetition rate of 50 Hz ($\sim 10^{-6}$ duty cycle). About 3×10^7 photons/pulse are available at the site of the sample. Spectra are recorded by sweeping the frequency of the dye-laser and monitoring the L_α transmission signal with a photodiode behind the sample in the experimental cell (see fig. 1).

Optical cooling of magnetically trapped H is conveniently described by considering the energy balance of an ensemble of atoms before and after the scattering of photons, using a formalism as given by Wineland and Itano [44]. The difference in internal energy of the sample per scattered photon (after averaging over the direction of the scattered photons) is given by $\Delta U = \hbar \boldsymbol{k} \cdot \boldsymbol{v} + 2E_r$, where $\boldsymbol{v}$ is the initial velocity of the atom, $\boldsymbol{k}$ the wavevector of the incident light ($k = 2\pi/\lambda$) and $E_r = \hbar^2 k^2 / 2m$ the photon-recoil energy. For H atoms excited at Lyman-α $E_r \approx 0.6$ mK. To obtain cooling the momentum vectors of atom and photons should be in opposite directions (red detuning). The effect is illustrated in fig. 3, where we show the π_1 and σ_1 lines as part of the transmission spectrum, recorded before and after irradiating the sample for 15 min at the indicated frequency ν_1 in the red wing of the σ_1-line. The fitted curves indicate Doppler cooling from 80(10) to 11(2) mK accompanied by an increase of n_0 by a factor 16 from $n_0 = 8(2) \times 10^{10}\,\mathrm{cm}^{-3}$ to $n_0 = 1.3(4) \times 10^{12}\,\mathrm{cm}^{-3}$. For the cooling only a single L_α beam is used, relying on elastic collisions between the trapped atoms to obtain three-dimensional cooling. Due to use of pulsed radiation the cooling proceeds in minutes rather than millisec-

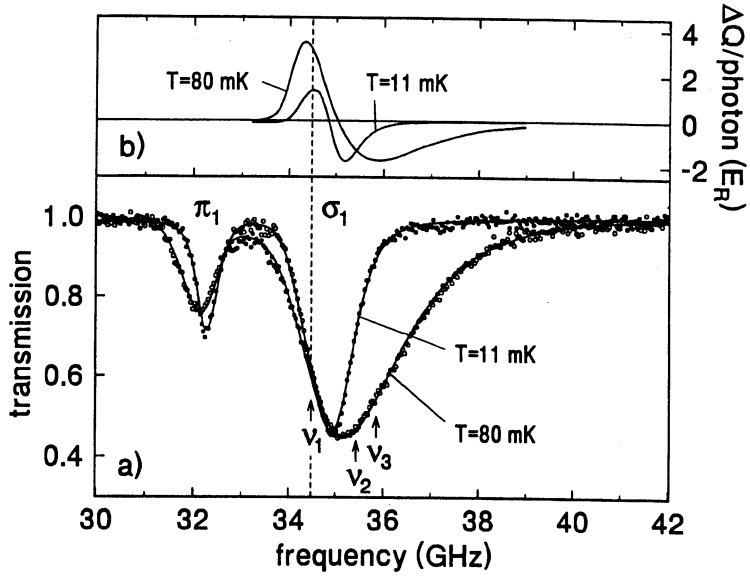

Fig. 3. (a) Transmission spectra before (open circles) and after (closed circles) Doppler cooling. The solid lines are calculated spectra for $T = 80(10)$ mK, $n_0 = 8(2) \times 10^{10}\,\mathrm{cm}^{-3}$ and $T = 11(2)$ mK, $n_0 = 1.3(4) \times 10^{12}\,\mathrm{cm}^{-3}$, respectively. (b) Cooling efficiency per scattered photon in recoil units (E_r).

onds (as usual in optical cooling experiments), i.e. in a time long in comparison with the interatomic collision rate but shorter than the sample life time at the quoted density. Hence the sample remains close to internal thermal equilibrium as in the case of evaporative cooling.

For a closed optical pumping cycle and neglecting multiple scattering the local rate of change of internal energy of the sample due to Doppler cooling at frequency $\omega = ck$ may be written (after integration over the thermal velocity distribution) in the following form:

$$\mathrm{d}\dot{U}(\omega, \boldsymbol{r}) = 2E_r \frac{I(\omega, \boldsymbol{r})}{\hbar\omega}\left(1 - \frac{k_B T}{\hbar}\frac{\partial}{\partial\omega}\right) n(\boldsymbol{r})\sigma(\omega, \boldsymbol{r})\mathrm{d}^3 r, \tag{17}$$

where $I(\omega, \boldsymbol{r})$ is the intensity profile of the incident light beam, $\sigma(\omega, \boldsymbol{r})$ is the atomic cross section for scattering L_α photons of frequency ω at position $\boldsymbol{r}$ and $n(\boldsymbol{r})\sigma(\omega, \boldsymbol{r}) = k\,\mathrm{Im}(\boldsymbol{\varepsilon}^* \cdot \vec{\vec{\chi}} \cdot \boldsymbol{\varepsilon})$ is the local extinction coefficient, with $\boldsymbol{\varepsilon}$ the polarization vector and

$$\vec{\vec{\chi}} = \mathrm{i}\frac{6\pi^{3/2}}{k^3}\sum_{h,l} n_h(\boldsymbol{r})\frac{\mathbf{D}_{hl} : \mathbf{D}_{hl}^*}{\sum_{h'} |\mathbf{D}_{h'l}|^2}\frac{\Gamma}{2b} w(\zeta) \tag{18}$$

the susceptibility tensor. In eq. (18) Γ is the natural linewidth, $b = k(2k_B T/m)^{1/2}$ a measure for the Doppler broadening, $\mathbf{D}_{hl}$ the electric dipole transition matrix ele-

ment between ground-state (hyperfine) level h and excited state level l, and $n_h(r)$ the partial density of h-state atoms. The real part of the complex error function $w(\zeta) \equiv e^{\zeta^2}\,\mathrm{erfc}(-i\zeta)$ with $\zeta \equiv (\omega - \omega_{lj} + i\Gamma/2)/b$ is the Voigt profile describing a Doppler-broadened line. The first term between the parentheses in eq. (17) describes the heating due to photon recoil and the second term the Doppler cooling. For optically thin samples the L_α beam is virtually unattenuated, i.e. the beam profile is frequency independent, $I(\omega, r) = I(r)$, and eq. (17) may be rewritten as

$$\dot{U}(\omega) = \frac{2E_r}{\hbar\omega}\left(1 - \frac{k_B T}{\hbar}\frac{\partial}{\partial\omega}\right)P(\omega), \tag{19}$$

where $P(\omega) \equiv \int I(r)n(r)\sigma(\omega, r)\,d^3r$ is the power removed from the L_α beam at frequency ω (absorption spectrum). For optimal cooling in low density samples the frequency should be tuned to the position of maximum derivative in the red wing of the σ_1 line. For free atoms the lowest temperature achievable with Doppler cooling is $T = \frac{1}{2}\hbar\Gamma/k_B \approx 2.4$ mK. Due to Zeeman broadening in the inhomogeneous trapping field, this Doppler limit is slightly increased, to 3.1 mK in the configuration of ref. [13].

A complication that applies to H but most likely not to $\bar{H}$ is that gas density is usually so high that the samples are optically thick at Lyman-α. Then, the Doppler limit is further increased by multiple scattering and relaxation heating. Eq. (19) is no longer valid and one has to rely on numerical integration of eq. (17). In this way the energy transfer per scattered photon versus frequency, shown in fig. 3, was calculated. The trajectory in the T-n_0 plane, recorded during Doppler cooling is shown in fig. 4 and compared to a curve obtained for constant particle number. Cooling is accompanied by compression in accordance with eq. (8). The initial deviation from the theoretical curve, above 50 mK, is caused by some additional cooling due to the evaporation mechanism. Towards the end of the cooling period a further increase in density is opposed by two loss mechanisms, spurious optical pumping to H ↓ and dipolar relaxation. Both the relaxation heating and particle loss are observed by letting the sample evolve in the dark for 37 min after the cooling period is terminated (see dash-dotted line in fig. 4). By applying Doppler cooling once more, the sample is subsequently cooled to $T \approx 8$ mK, close to its theoretical limit.

In summary, Doppler cooling may be valuable to cool $\bar{H}$, without loss of sample, from the trapping temperature (~ 1 K) to temperatures $T < 10$ mK, close to the Doppler limit. This may be of interest to reduce second-order broadening in precision spectroscopic studies or to simply reduce the sample size. It may also serve as a first stage before cooling to sub-Doppler temperatures by evaporative or adiabatic cooling. For $T \gtrsim 10$ mK it is very unlikely that thermodynamic samples may be produced. Therefore, the cooling of the anti-atoms has to proceed independently, not necessarily a handicap as long as the orbital degrees of freedom are coupled and the particles samples the whole trap. This coupling between degrees of freedom has been studied by Shlyapnikov et al. [14] in relation to one-dimensional

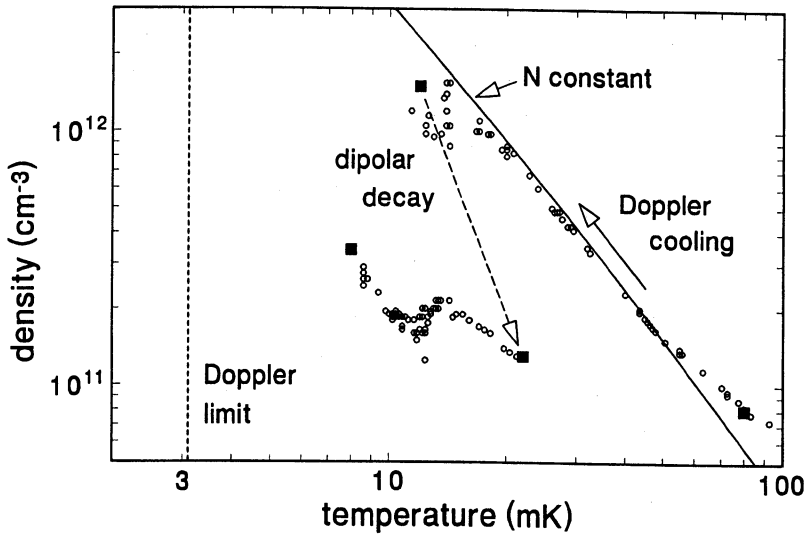

Fig. 4. Cooling trajectories in the T–n_0 plane. Doppler cooling data compared to a constant-atom-number trajectory (solid line). The dipolar decay and heating during a 37 min period is indicated by the dashed line.

adiabatic cooling. It was found to be substantial in Ioffe traps for $T \gg T_0$. To calculate the cooling rate eq. (17) cannot be used as it presumes a thermal velocity distribution. Accurate estimates of the cooling rate should be based on realistic velocity distributions of the trapped anti- atoms.

Acknowledgement

The author wishes to thank T.W. Hijmans, O.J. Luiten, I.D. Setija, H.G.C. Werij, M.W. Reynolds, R. van Roijen, J.J. Berkhout and S. Jaakkola for their contributions to the hydrogen trapping experiments in Amsterdam. The financial support of the Nederlandse Organisatie voor Wetenschappelijk Onderzoek (NWO-PIONIER), de Stichting FOM and the EC-SCIENCE program is gratefully acknowledged.

References

[1] G. Gabrielse, X. Fei, K. Helmerson, S. Rolston, R.J. Tjoelker, T.A. Trainor, H. Kalinowsky, J. Haas and W. Kells, Phys. Rev. Lett. 57 (1986) 2504.

[2] G. Gabrielse, X. Fei, L.A. Orozco, R.J. Tjoelker, J. Haas, H. Kalinowsky, T.A. Trainor and W. Kells, Phys. Rev. Lett. 63 (1989) 1360.

[3] G. Gabrielse, X. Fei, L.A. Orozco, R.J. Tjoelker, J. Haas, H. Kalinowsky, T.A. Trainor and W. Kells, Phys. Rev. Lett. 65 (1990) 1317.
[4] Hyp. Int., several papers in this volume.
[5] A.P. Mills, Hyp. Int., this volume.
[6] G. Gabrielse, S.L. Rolston, L. Haarsma and W. Kells, Phys. Lett. A129 (1988) 38.
[7] R.J. Hughes, Hyp. Int., this volume.
[8] H.F. Hess, G.P. Kochanski, J.M. Doyle, N. Masuhara, D. Kleppner and T.J. Greytak, Phys. Rev. Lett. 59 (1987) 672.
[9] R. van Roijen, J. Berkhout, S. Jaakkola and J.T.M. Walraven, Phys. Rev. Lett. 61 (1988) 931.
[10] N. Masuhara, J.M. Doyle, J.C. Sandberg, D. Kleppner, T.J. Greytak, H.F. Hess and G.P. Kochanski, Phys. Rev. Lett. 61 (1988) 935.
[11] J.M. Doyle, J.C. Sandberg, I.A. Yu, C.L. Cesar, D. Kleppner and T.J. Greytak, Phys. Rev. Lett. 67 (1991) 603.
[12] O.J. Luiten, H.G.C. Werij, I.D. Setija, M.W. Reynolds, T.W. Hijmans and J.T.M. Walraven, Phys. Rev. Lett. 70 (1993) 544.
[13] I.D. Setija, H.G.C. Werij, O.J. Luiten, M.W. Reynolds, T.W. Hijmans and J.T.M. Walraven, Phys. Rev. Lett,, submitted.
[14] G.V. Shlyapnikov, J.T.M. Walraven and E.L. Surkov, Hyp. Int., this volume.
[15] T.W. Hänsch, Hyp. Int., this volume.
[16] D. Kleppner, in: *The Hydrogen Atom*, eds. G.F. Bassini, M. Inguscio and T.W. Hänsch (Springer, Berlin, 1989) p. 103.
[17] T.W. Hänsch, in: *The Hydrogen Atom*, eds. G.F. Bassini, M. Inguscio and T.W. Hänsch (Springer, Berlin, 1989) p. 93.
[18] F. Schmidt-Kaler, T. Andreae, W. König, D. Leibfried, L. Ricci, M. Weitz, R. Wynands, C. Zimmermann and T.W. Hänsch, At. Phys. 13, in press (ICAP-13).
[19] G. Gabrielse, Hyp. Int. 44 (1988) 349.
[20] N. Beverini, V. Lagomarsino, G. Manuzio, F. Scuri and G. Torelli, Hyp. Int. 44 (1988) 357.
[21] K.-J. Kügler, W. Paul and U. Trinks, Phys. Lett. 72B (1978) 422.
[22] A.L. Migdall, J.V. Prodan, W.D. Phillips, T.H. Bergeman and H.J. Metcalf, Phys. Rev. Lett. 54 (1985) 2596.
[23] J.V. Prodan, A.L. Migdall, W.D. Phillips, I. So, H.J. Metcalf and J. Dalibard, Phys. Rev. Lett. 54 (1985) 992.
[24] V.S. Bagnato, G.P. Lafyatis, A.G. Martin, E.L. Raab, R.N. Ahmad-Bitar and D.E. Pritchard, Phys. Rev. Lett. 58 (1987) 2194.
[25] D.E. Pritchard, Phys. Rev. Lett. 51 (1983) 1336.
[26] S. Chu, J.E. Bjorkholm, A. Ashkin and A. Cable, Phys. Rev. Lett. 57 (1986) 314.
[27] I.F. Silvera and J.T.M. Walraven, Phys. Rev. Lett. 44 (1980) 164.
[28] H.F. Hess, Phys. Rev. B34 (1986) 3476.
[29] P.D. Lett, P.L. Gould and W.D. Phillips, Hyp. Int. 44 (1988) 335.
[30] W.D. Phillips and S.L. Rolston, Hyp. Int., this volume.
[31] W.H. Wing, Prog. Quant. Electron. 8 (1984) 181.
[32] R.V.E. Lovelace, C. Mehanian, T.J. Tommila and D.M. Lee, Nature 318 (1985) 30.
[33] F.G. Major and H.G. Dehmelt, Phys. Rev. 170 (1968) 91.
[34] E.A. Cornell, C. Monroe and C.E. Wieman, Phys. Rev. Lett. 67 (1991) 2439.
[35] C.C. Agosta, I.F. Silvera, H.T.C. Stoof and B.J. Verhaar, Phys. Rev. Lett. 62 (1989) 2361.
[36] R.J.C. Spreeuw, private communication.
[37] T. Bergeman, G. Erez and H.J. Metcalf, Phys. Rev. A35 (1987) 1535.
[38] T. Bergeman, P. McNicholl, J. Kycia, H. Metcalf and N.L. Balazs, J. Opt. Soc. B6 (1989) 2249.
[39] Y.V. Gott, M.S. Ioffe and V.G. Tel'kovskii, Nucl. Fusion, 1962 suppl., Pt. 3 (1962) 1045.
[40] A. Lagendijk, I.F. Silvera and B.J. Verhaar, Phys. Rev. B33 (1986) 626.
[41] H.T.C. Stoof, J.M.V.A. Koelman and B.J. Verhaar, Phys. Rev. B38 (1988) 4688.

[42] T.W. Hänsch and A.L. Schawlow, Opt. Commun. 13 (1975) 68.
[43] D. Wineland and H. Dehmelt, Bull. Am. Phys. Soc. 20 (1975) 637.
[44] D.J. Wineland and W.M. Itano, Phys. Rev. A20 (1979) 1521.
[45] K. Helmerson, A. Martin and D.E. Pritchard, J. Opt. Soc. Am. B9 (1992) 483.
[46] K. Helmerson, A. Martin and D.E. Pritchard, J. Opt. Soc. Am. B9 (1992) 1988.
[47] T.W. Hijmans, O.J. Luiten, I.D. Setija and J.T.M. Walraven, J. Opt. Soc. Am. B6 (1989) 2235.
[48] H.G.C. Werij, O.J. Luiten, I.D. Setija, T.W. Hijmans and J.T.M. Walraven, to be published.